A Micromechanical Numerical Analysis for a Triaxial Compression of Granular Materials

V. Magnanimo* and L. La Ragione†

*Multi Scale Mechanics (MSM), Faculty of Engineering Technology,
University of Twente, P.O. Box 217, 7500 AE Enschede, The Netherlands.
†Dipartimento di Scienze dell'Ingegneria Civile e dell'Architettura,
Politecnico di Bari, 70125 Bari, Italy.

Abstract. We focus on a triaxial compression at constant pressure in which a granular material, after an isotropic preparation, is sheared in a small range of monotone deformation. The aggregate is made by identical, elastic, spheres that interact through a non central contact forces. Because of the loading condition the material is transversely isotropic. Through a numerical analysis we show that aggregates with same pressure and porosity behave differently depending on the initial coordination number (i.e. the average number of contacts per particle). The relation of stress, volume change, elastic moduli and microstructure with the initial contact network is investigated.

Keywords: DEM, Anisotropy, Microstructure
PACS: 45.70.Cc, 81.05.Xj, 81.05.Rm

INTRODUCTION

Granular materials, in nature, are essentially anisotropic. We typically deal with an induced and/or inherent anisotropy. The former is associated with the loading conditions, the latter occurs because of the particulate nature of the material that can show preferential directions in the contact network. In both cases anisotropy is an important ingredient of any constitutive law for granular materials. In the past years, numerical simulations (e.g. [1, 2]), theoretical analysis (e.g. [3, 4, 5]) and physical experiments (e.g. [6, 7, 8]) have been able to capture some features associated with anisotropy in phenomena like dilatancy, shear bands, wave propagation or ratcheting [9]. An interesting open issue concerns the essential state variables needed to describe the anisotropic aggregate. Conventional approaches in the framework of solid-state elasticity consider the response to be dependent on the solid volume fraction and the stress state. On the other hand, micromechanics has supported the idea that along with macroscopic properties, the response of an aggregate is characterized by the fabric tensors and the coordination number [13, 14, 8, 18]. The former refers to the geometric arrangement of the contacts, the latter is the (scalar) average number of contacts per particle.

Here we follow the micromechanical approach and investigate the influence of the coordination number on the behavior of the anisotropic granular material. We consider an ideal aggregate made by identical, frictional, elastic spheres. We employ a numerical protocol that is able to generate isotropic packings with constant pressure and solid volume fraction but different coordination numbers [13, 14]. We subsequently apply an axial-symmetric compression at constant pressure to the different packings. We focus on a regime of deformation where the deviatoric strain is small compared to the isotropic strain associated with its compression. In this range, we can assume that deformations are homogeneous [10] with a value of the stress rather high, close to the peak [11]. Moreover, due to the induced anisotropy, the effective moduli show a not negligible evolution with respect to their initial values [12]. We analyze the dependence of the response on the initial configuration fully characterized by the isotropic structure. We find that deviatoric stress, volume change, coordination number, as well as the contact orientation, evolves differently with the shear strain depending on the initial coordination number k_0 of the granular sample.

NUMERICAL SIMULATION

Initial isotropic state. We perform DEM simulations [15, 16] on random assemblies of identical, frictional, elastic spheres. Our numerical experiments consider $N = 10,000$ particles, each with diameter $d = 0.2$ mm, randomly generated in a periodic cubic cell. We employ material properties typical of glass spheres: shear modulus $\mu = 29$GPa and Poisson's ratio, $\nu = 0.2$. The static friction coefficient is set to $\mu_s = 0.3$. The interaction between particles is given by a non-central contact force in which the normal component follows the non-linear Hertz interaction. The tangential component is bilinear and it incorporates elastic displacement and frictional sliding.

Powders and Grains 2013
AIP Conf. Proc. 1542, 1234-1237 (2013); doi: 10.1063/1.4812161

After random generation, particles are isotropically compressed in the absence of gravity from an initial gas to the desired solid volume fraction. Because we are interested in dense aggregates of frictional particles, we require that the solid volume fraction ϕ is close to the random close packing value $\phi_{RCP} \simeq 0.64$. It is well known that different packing structures are obtained experimentally according to the preparation protocol [17, 18]. Our approach is to generate numerical packings with different final structure. To do this we employ a protocol where ϕ and p are set in two different stages of the deformation (details are given in [13]). The result is that, for a given pressure ($p = 100$kPa) and identical solid volume fraction ($\phi \simeq 0.638$), we obtain isotropic packings with different coordination number; here we consider three aggregates with $k_0 = 6.17, 5.36, 4.88$ and volumetric strain $\Delta_0 = 7.59\text{x}10^{-4}, 8.96\text{x}10^{-4}, 9.93\text{x}10^{-4}$, respectively.

RESULTS

Axialsymmetric compression. The three samples described above are subjected to axisymmetric deformation with $\hat{\mathbf{h}} = \mathbf{e_3}$ as direction of the major (compressive) principal strain. The test is carried out at constant mean stress $p = p_0 = 100$ kPa [1]. During each loading step, the target pressure is maintained with a servo mechanism which continuously adjusts the applied strain rate according to the difference between the desired stress state and the stress measured at that time step [13]. We want to reproduce a quasi-static, triaxial loading so we compress the sample very slowly ($\gamma_{\partial t}/\Delta_0$ is lower than 5×10^{-3}, where $\gamma_{\partial t}$ is the accumulated strain in the time step ∂t). After each increment we let the system to relax until a new equilibrium state is reached.

In Figs. 1a, 1b and 1c we plot the evolution of the normalized deviatoric stress, volumetric strain and coordination number during the deviatoric path. Hereafter we normalize the deviatoric strain with the initial isotropic volume, Δ_0. Although each sample maintains the same confining pressure, the volume strain is different because the initial coordination number, k_0, varies. The deviatoric stress is defined as

$$\frac{q}{p_0} = \frac{1}{2p_0}\left[\frac{\sigma_{11}+\sigma_{22}}{2} - \sigma_{33}\right], \qquad (1)$$

where σ_{ii} are the diagonal components of the average stress tensor $\boldsymbol{\sigma}$ obtained from the simulation [2].

In the figures we observe three different curves, depending on the initial value k_0. During the deformation ϕ remains almost constant while the pressure is kept constant; that is the behavior of the aggregate depends on the initial microstructure through k_0. The stress increases faster for higher initial coordination number, as it leads

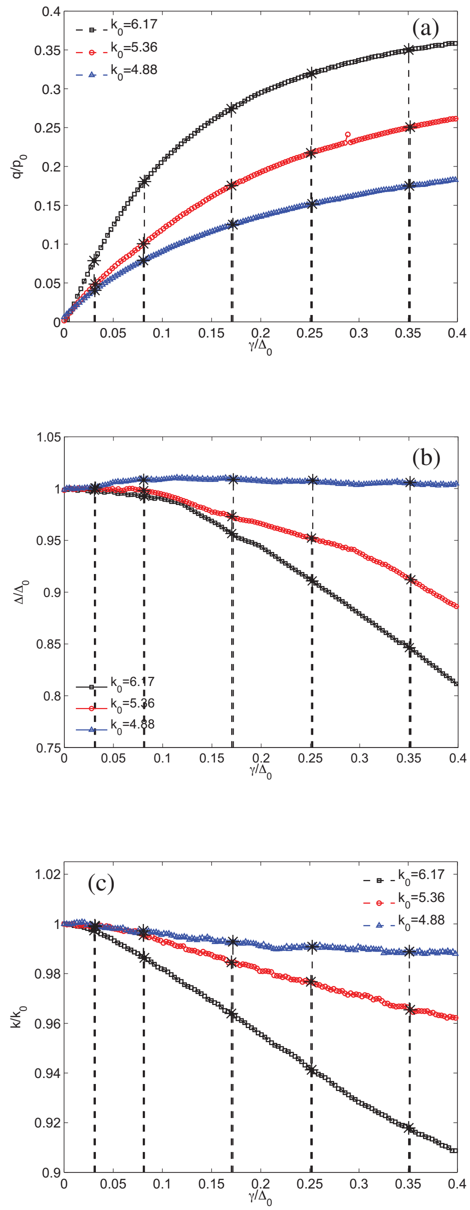

FIGURE 1. Normalized (a) deviatoric stress, (b) volumetric strain and (c) coordination number versus normalized deviatoric strain for different initial coordination numbers k_0. The black stars indicate the points where the shear moduli (Fig. 2) are calculated.

to higher initial shear resistance [13, 14]. The volumetric strain (Fig. 1b) and the coordination number (Fig. 1c) behave in a similar fashion, their variation being faster for higher k_0. Interestingly, the less connected sample ($k_0 = 4.88$) contracts rather then dilate and preserves al-

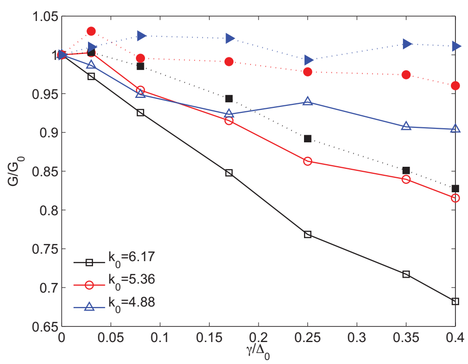

FIGURE 2. Evolution of the shear moduli with the normalized deviatoric strain for samples with different initial coordination number k_0. Solid lines with empty symbols, dotted lines with filled symbols denote G_{12} and $G_{13} = G_{23}$ respectively.

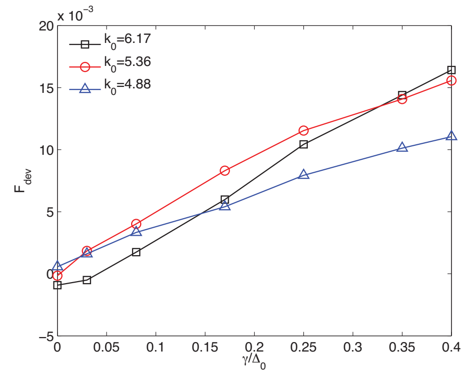

FIGURE 3. Evolution of the deviatoric fabric with the normalized deviatoric strain for samples with different initial coordination number k_0.

most the same number of contacts.

Shear Moduli. At different steps along the loading path (see black stars in Fig.1), the shear moduli of the aggregate are calculated applying an incremental strain and measuring the corresponding incremental stress response [19, 13]. The transversal and axial shear moduli are respectively $G_{12} = \Delta\sigma_{12}/\Delta\varepsilon_{12}$ and $G_{13} = G_{23} = \Delta\sigma_{23}/\Delta\varepsilon_{23}$, where ε_{ij} are components of the strain tensor. The friction coefficient is set on a very high value to prevent sliding between grains because we are interested in the elastic resistance of the aggregate.

In Fig. 2 we report the evolution of the shear moduli with respect to the initial isotropic value G_0, for samples characterized by $k_0 = 6.17, 5.36$ and 4.88. The response depends on the initial microstructure through k_0 and the evolution of the coordination number k that differs in the three samples (see Fig.1c). The more contacts are lost, the faster the moduli decrease. Interestingly, for all the three samples, the modulus in the transversal isotropic plane G_{12} varies faster than the axial shear modulus G_{13} (in particular, G_{13} stays almost constant in the case $k_0 = 5.36$ and 4.88). This is reasonable since deletion mostly affects pairs of particles with contact vectors in the equatorial plane [3]. So, due to the loss of contacts, the material can be sheared more easily in the isotropic plane.

Microstructure. Finally we carry out DEM simulation to investigate the modification of the contact network during the axial-symmetric compression. It is known that a granular material becomes anisotropic when sheared. Partly this is due to contacts lost in the minor principal strain direction, i.e. the geometric fabric changes [20]. But also, when contacts obey the Hertzian law, they become stiffer in the major direction and softer in the minor direction, depending on the angular force distribution [3]. If no particular boundary condition are used, both geometric and stiffness effects occur during the axial-symmetric compression. We want to distinguish between the two effects. We focus on the fabric tensor [20] defined as

$$F_{ij} = \frac{1}{N^c} \sum_{c=1}^{N^c} \hat{d}_i^c \hat{d}_j^c, \qquad (2)$$

where N^c is the total number of contacts in the aggregate and $\hat{\mathbf{d}}^c$ are direction cosines of the c-th contact. The second order tensor $\mathbf{F}$ is symmetric and its trace is equal to 1. While k is a measure of the contacts density in the aggregate, the fabric tensor $\mathbf{F}$ provides information on the spatial distribution of the contacts through its eigenvalues. In order to study the evolution of the geometric anisotropy in the samples, we calculate the eigenvalues F_{ii} of $\mathbf{F}$ and the deviatoric fabric in the anisotropic states (stars in Fig.1) as $F_{dev} = [F_{33} - (F_{11} + F_{22})/2]/2$. Results in Fig.3 show that F_{dev} evolves with strain, with a slight difference between the sample at lower k_0 and the other two.

We also scrutinize the evolution of the contact stiffness in different directions during the deformation. We define the average contact stiffness as

$$\langle K_N \rangle_{\hat{\mathbf{d}}} = \frac{1}{M^p} \sum_{\mathbf{d}^{(AB)} \subset \Delta\Omega^p} K_N^{(AB)}, \qquad (3)$$

where $K_N^{(AB)}$ is the normal stiffness for a contacting pair AB within the element of solid angle centered on $\hat{\mathbf{d}}^p$ and M^p is the number of pairs in that solid angle $\Delta\Omega$ (see [21]). In the initial, isotropic state, $\langle K_N \rangle_0$ is independent of the direction $\hat{\mathbf{d}}^p$. We introduce the contact stiffness

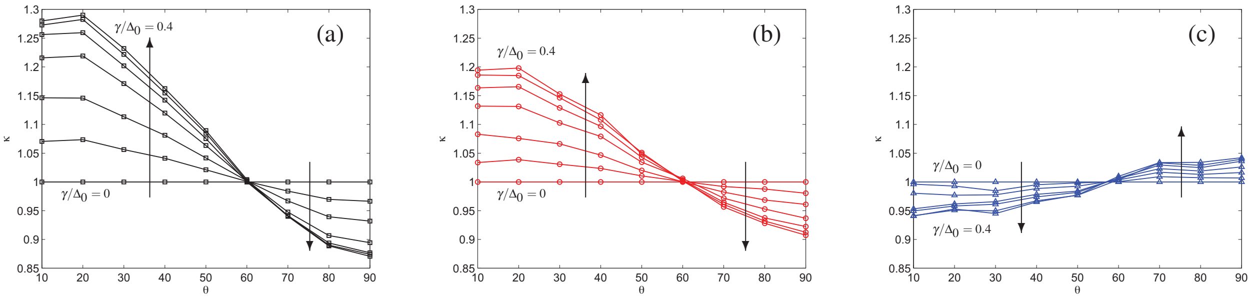

FIGURE 4. Stiffness ratio κ versus polar angle with γ/Δ_0 that varies from 0 to 0.4, for samples with different initial coordination number. In all figures black squares, red circles and blue triangles correspond to $k_0 = 6.17, 5.36$ and 4.88 respectively.

ratio as

$$\kappa = \frac{\langle K_N \rangle_{\hat{\mathbf{d}}}}{\langle K_N \rangle_0} \quad (4)$$

in order to quantify the evolution of the κ with respect to the initial reference state. In Fig. 4 we plot κ with $\hat{\mathbf{d}}^p$ oriented along a given θ every 10° in the interval $0^\circ - 90^\circ$. With increasing γ/Δ_0 and for $k_0 = 6.17$ and $k_0 = 5.36$, κ increases in the axial direction (0°) and decreases in the proximity of the horizontal isotropic plane (90°). At about 60°, with $\kappa = 1$, we find the angle where the overlap between contacting particles does not change with the strain. This is a "neutral" direction of contacts in the triaxial test. Interestingly, for $k_0 = 4.88$ (Fig. 4c), κ shows an opposite trend with respect to the highly coordinate aggregates. Moreover, a much smaller variation of κ (in magnitude) is observed for this sample, in agreement with the behavior of the macro-quantities in Fig. 1 and the effective moduli (Fig. 2). The neutral direction stays at about 60° also in this last case.

CONCLUSIONS

In the small range of deformation that precedes the stress peak, we investigate the influence of the initial isotropic structure on the subsequent deviatoric behavior of a granular assembly. The initial structure seems to play a crucial role with respect to the evolution of stress, volumetric strain and coordination number itself during the axialsymmetric deformation. Interestingly, when looking at the microstructure, we find that the value of the coordination number in the isotropic configuration determines how the anisotropic contact network evolves with shearing. Consequently, the shear resistance in axial/horizontal direction is affected by the initial state. The poorly coordinate aggregate shows a very peculiar behavior with respect to the highly coordinated ones ($k_0 = 5.36$ and $k_0 = 6.17$), its features resembling the response of loose rather than dense samples.

REFERENCES

1. C. Thornton, and S. J. Antony, *Roy Soc of London Phil Tr A* **356**, 2763 (1998).
2. S. Luding, *J. Phys.: Condens. Matter* **17**, S2623–S2640 (2005).
3. J. Jenkins, and O. Strack, *Mechanics of Materials* **16**, 25–33 (1993).
4. F. Nicot, and F. Darve, *Mechanics of Materials* **37**, 980–1006 (2005).
5. C. Chang, and Z. Yin, *Mechanics of Materials* **136**, 830–839 (2012).
6. R. Kuwano, and R. J. Jardine, *Géotechnique* **52**, 727 (2002).
7. Y. Khidas, and X. Jia, *Phys. Rev. E* **81**, 21303 (2010).
8. A. Ezaoui, and H. D. Benedetto, *Géotechnique* **59**, 621–635 (2009).
9. V. Magnanimo, and S. Luding, *Granular Matter* **13**, 225–232 (2011).
10. C. Thornton, and L. Zhang, *Philosophical Magazine* **86**, 3425–3452 (2006).
11. A. S. J. Suiker, and N. A. Fleck, *J. Appl. Mech.* **71**, 350–358 (2004).
12. L. L. Ragione, and V. Magnanimo, *Granular Matter* **14**, 749–757 (2012).
13. V. Magnanimo, L. L. Ragione, J. Jenkins, P. Wang, and H. Makse, *EPL (Europhysics Letters)* (2008).
14. I. Agnolin, and J. Roux, *Phys. Rev. E* **76**, 061304 (2007).
15. P. A. Cundall, and O. D. L. Strack, *Géotechnique* **29**, 47–65 (1979).
16. S. Luding, “Molecular Dynamics Simulations of Granular Materials,” in *The Physics of Granular Media*, edited by H. Hinrichsen, and D. E. Wolf, Wiley VCH, Weinheim, Germany, 2004, pp. 299–324.
17. E. R. Nowak, J. B. Knight, E. Ben-Naim, H. M. Jaeger, and S. R. Nagel, *Phys. Rev. E* **57**, 1971–1982 (1998).
18. J. Yang, Z. X. Yang, and X. S. Li, *Géotechnique* **58**, 237–248 (2008).
19. H. A. Makse, N. Gland, D. L. Johnson, and L. Schwarz, *Phys. Rev. E* **70**, 061302 (2004).
20. M. Oda, S. Nemat-Nasser, and J. Konishi, *Soils and Foundation* **25**, 13 (1985).
21. J. Jenkins, D. Johnson, L. L. Ragione, and H. Makse, *J. Mech. Phys. Solids* **53**, 197–225 (2005).